Continuous Second-order Sliding Mode Control Based on Disturbance Observer for LOS Stabilized System

Jianliang Mao Shihua Li Qi Li Jun Yang
School of Automation, Southeast University, Nanjing 210096, China
Key Laboratory of Measurement and Control of Complex Systems of Engineering, Ministry of Education, Nanjing 210096, China
Email: lsh@seu.edu.cn

***Abstract*—This paper develops a continuous second-order sliding mode control based on finite-time disturbance observer for light of sight (LOS) stabilized loop of inertial stabilized platform. The main purpose of an inertial stabilized platform is to eliminate the various disturbances to make the LOS keep steady in an inertial space. To accomplish the controller design, the equations of motion for a 2-DOF gimbal system driven by permanent synchronous motors are established and the cross coupling torque, mass unbalance torque, uncertain load torque are treated as the lumped disturbances. And to improve the tracking accuracy, a new continuous sliding mode control approach is employed to control the rate loop of the system. The proposed method confirms that the tracking error of LOS rate converges to zero in finite time even in the presence of the disturbances. By using the Lyapunov function technique, a rigorous finite-time convergence proof is given. The comparison simulation results show that the proposed method for LOS stabilized system exhibits a promising control performance in practical engineering.**

I. Introduction

The optical electronic tracking system plays an important role in aerospace applications. A LOS stabilized platform is usually utilized to maintain the sightline of an optical sensor relative to anther object or inertial space with the external disturbances, such as vehicle motion or vibration, which also called inertial stabilized platform (ISP) [1]. Basic stabilization is usually accomplished by fixing the sensor in a 2-DOF gimbal system, with the sensor on the inner gimbal. With the disturbances, such as inertial crossing coupling, friction, mass unbalance, parameter variations and uncertain load, an ISP belongs to a class of typical nonlinear and coupling system [2], [3], [7]. The high precision tracking and anti-disturbances control have been an challenging task.

At present, robust control and decoupling control methods are still widely used for ISP in application [3], [4], [5], [6], [7]. Throughout the above control methods, it is powerful to handle the system disturbances constrained to be slowly time-varying or constant ones. However, the designed stable controllers can hardly meet the demand of fast frequency response and high precision tracking in the presence of the disturbances with sinusoidal or slope forms. In addition, almost all studies presented above take DC torque motor as actuator which is widely utilized in an ISP system. And there are many shortcomings in DC motor on performance and maintenance. Permanent magnet synchronous motor (PMSM) has gained a wide acceptance in motion control applications due to its high performance [8]. Due to the strong coupling characteristics of PMSM itself, many nonlinear control methods have been developed, such as adaptive control [9], sliding mode control [10], disturbance-observer control [11]. These approaches have made the contributions on improving the performance of the motor from various aspects.

Due to the insensitivity to model uncertainties and parameter variations, the sliding mode control (SMC) has been widely used in guidance and tracking system so as to achieve the robustness against the disturbances. The undesired result is the control chattering which will cause plenty of noise and ripple in many practical application system [12]. Continuous sliding mode control has been proposed to reduce chattering by using many effective methods. In [13], finite time control (FTC) methods based on terminal sliding mode (TSM) is presented for robotic manipulators. However, it constrains the sliding system's trajectories not to the sliding surface but to its vicinity, which loses the robustness and rejection to disturbances. Disturbance observer-based (DOB) has been proved to be effective in compensating for the effects of unknown external disturbances [14], [15]. A second-order sliding mode control (SOSMC) based on disturbance observer is proposed to achieve enhanced tracking accuracy with a finite-time convergence in [16], avoiding the existing problem in [13]. And the continuous sliding mode control approaches based on finite-time disturbance observer (FTDO) are also presented by [17], [18]. Another method for reducing chattering is high-order sliding mode control [19], [16], [20]. For a system with relative degree one, super-twisting (STW) algorithm has been proved to be effective in disturbance rejection. But the limitation is that it requires the knowledge of the boundary of the disturbance gradient.

In this paper, we first adopt PMSM into an ISP system with no motor reducer, and equations of motion for a 2-DOF gimbal system considering mass unbalance and vehicle motion are established. Second, a continuous second order sliding

978-1-4673-9788-9/16/$31.00 ©2016 IEEE

mode control scheme based on disturbance compensation is developed to ensure that the angular rate tracking error of LOS converge to zero in finite time.

The proposed methods exhibits the following attractive features. First, the external disturbances such as cross coupling torque, mass unbalance and uncertain load torque are estimated by FTDO in finite time, which can be periodic and not just slowly time-varying or constant. Second, the boundary of disturbance gradient is not necessary for the gain coefficient, so the overshooting of states can be avoided by the relative small control energy. Third, the proposed control method is continuous such that the chattering phenomenon will be attenuated and the angular rate tracking error will converge to zero in the presence of unknown bounded disturbances in finite time.

II. Model Description

Due to the vehicle motion or vibration, the LOS of optical electronic tracking system will deviate from the target location under the cross coupling torque and external load torque. By fixing the sensor in the inner gimbal of 2-DOF ISP system, the LOS stabilization can be accomplished in the presence of disturbances on pitch and yaw channels. And the gyro signals are utilized as feedback to form the rate stable loop.

A. Dynamics Model of 2-DOF Gimbal

A typical two-axis, pitch-yaw system's structure can be seen in [2]. To simplify the description, the same coordinate definition has been used, that is the gimbal platform or base frame B, followed by the gimbal mediator or outer frame K, and finally the inner frame A. For the angular rate of frames B, K, and A relative to inertial space, respectively, we introduce Ω_B, Ω_K and Ω_A, where $\Omega_B = [p, q, r]^{\mathrm{T}}$, $\Omega_K = [p_k, q_k, r_k]^{\mathrm{T}}$, $\Omega_A = [p_a, q_a, r_a]^{\mathrm{T}}$, where p, q, r are the components in frame B of the inertial angular rate vector, and the notations p, q, r for the roll, pitch and yaw components, respectively, similar definitions for other vectors. Then the angular rate kinematics of tow gimbals taking into account relative angles of rotation v_1, v_2 is given by

$$\Omega_K = R_b^k \cdot \Omega_B + \begin{bmatrix} 0 \\ 0 \\ \dot{v}_1 \end{bmatrix}, \Omega_A = R_k^a \cdot \Omega_K + \begin{bmatrix} 0 \\ \dot{v}_2 \\ 0 \end{bmatrix}. \quad (1)$$

where R_b^k, R_k^a are the transformations from B to K and K to A, respectively.

$$\begin{aligned} R_b^k &= \begin{bmatrix} \cos v_1 & \sin v_1 & 0 \\ -\sin v_1 & \cos v_1 & 0 \\ 0 & 0 & 1 \end{bmatrix}, \\ R_k^a &= \begin{bmatrix} \cos v_2 & 0 & -\sin v_2 \\ 0 & 1 & 0 \\ \sin v_2 & 0 & \cos v_2 \end{bmatrix}. \end{aligned} \quad (2)$$

The inertial matrices of the gimbals are denoted by

$$J_A = \begin{bmatrix} J_{ax} & D_{xy} & D_{xz} \\ D_{xy} & J_{ay} & D_{yz} \\ D_{xz} & D_{yz} & J_{az} \end{bmatrix}, J_K = \begin{bmatrix} J_{kx} & d_{xy} & d_{xz} \\ d_{xy} & J_{ky} & d_{yz} \\ d_{xz} & d_{yz} & J_{kz} \end{bmatrix}. \quad (3)$$

Then by Newton-Euler rotational equations, the basic equation of motion for pitch-yaw gimbals can be obtained as follows

$$\begin{aligned} J_{ay}\dot{q}_a &= T_y + T_B + T_C, \\ J_k\dot{r}_k &= T_z + T_b + T_c. \end{aligned} \quad (4)$$

A detailed derivation can be found in Appendix of [2]. T_y, T_z represent the total torque, including motor electromagnetic, friction torque and other disturbances torques. T_B and T_b represent the disturbances caused by body rotations, T_C and T_c are cross coupling terms.

To simply (4), the dynamic model can be redefined as follows

$$J(v_i)\dot{\omega}_i = T_{ei} + B_i\dot{v}_i + f(t, \omega_i, v_i), \quad (5)$$

where $i = 1, 2$ represent yaw and pitch channel respectively, v_i is the relative angle of rotation, $J(v_i)$ is the moment of inertial, ω_i is the absolute angular rate relative to inertial space of i channel. T_{ei} is the motor electromagnetic, B_i is the viscous friction coefficient, $f(t, \omega_i, v_i)$ are the crossing coupling torque and other unknown but continuous bounded disturbances which cannot be precisely modeled, e.g., external uncertain load torque, such as cable restraint, wind drag, et al.

B. Model of PMSM

The actuator we adopt here is a surface-mounted PMSM rather than a DC motor. Suppose that the three-phase stator windings of PMSM are sinusoidally distributed in space. For the purpose of control design, (i_d, i_q) are chosen as state variables. The PMSM system can be given in the following explicit form [8]

$$\begin{aligned} \dot{i}_d &= -\frac{R_s i_d}{L_d} + n_p\omega i_q + \frac{u_d}{L_d} \\ \dot{i}_q &= -\frac{R_s i_q}{L_q} - n_p\omega i_d + \frac{n_p\phi_v\omega}{L_q} + \frac{u_q}{L_q} \end{aligned} \quad (6)$$

where L_d and L_q denote the inductances of d-q axes, respectively. u_d, u_q and i_d, i_q are the d-axis and q-axis stator voltages and currents, respectively. R_s, n_p, ϕ_v present the stator resistance, the number of pole pair and the rotor flux linkage, ω is the rotor speed.

C. Rate-Current Cascade Control Models

For pitch gimbal, combing with (5) and (6), the integrated models are presented as follows

$$\begin{aligned} \dot{q}_a &= \frac{3}{2J_{ay}} n_p\phi_v i_q - \frac{B_2}{J_{ay}}(q_a - q_k) + \frac{f(t, q_a, v_2)}{J_{ay}}, \\ \dot{i}_d &= -\frac{R_s i_d}{L_d} + n_p(q_a - q_k) i_q + \frac{u_d}{L_d} \\ \dot{i}_q &= -\frac{R_s i_q}{L_q} - n_p(q_a - q_k) i_d + \frac{n_p\phi_v(q_a - q_k)}{L_q} + \frac{u_q}{L_q} \end{aligned} \quad (7)$$

where (q_a, i_d, i_q) are chosen as state variables, then the control objective is to keep $q_a = q_{ar}$, where q_{ar} is the desired angular rate, in the presence of various disturbances. A similar analysis and conclusion can be obtained for yaw gimbal.

In order to achieve a better dynamic performance, the field oriented control (FOC) technique is employed to decouple the

torque generation and the magnetization functions in PMSM. The detailed block diagram can be seen in [8]. In this strategy, the controller employs a structure of cascade control loops including a rate loop and two current loops. Suppose that i_q^* is the reference current of i_q current loop, then we can define current tracking error $\Delta i_q = i_q^* - i_q$. From (7), the first-order dynamics for outer rate loop and inner current loops can be given by

$$\dot{q}_a = g_\omega(q_a) + b_\omega i_q^* + d_\omega(t, q_a), \tag{8a}$$

$$\dot{i}_q = g_{i_q}(i_q) + b_{i_q} u_q + d_{i_q}(t, i_q), \tag{8b}$$

$$\dot{i}_d = g_{i_d}(i_d) + b_{i_d} u_d + d_{i_d}(t, i_d), \tag{8c}$$

where $g_\omega(q_a) = -\frac{B_2}{J_{ay}} q_a$, $b_\omega = \frac{3}{2J_{ay}} n_p \phi_v$, $d_\omega(t, q_a) = -\frac{B_2}{J_{ay}} q_k + \frac{f(t, q_a, v_2)}{J_{ay}} - \frac{3}{2J_{ay}} n_p \phi_v \Delta i_q$, $g_{i_q} = -\frac{R_s i_q}{L_q}$, $b_{iq} = \frac{1}{L_q}$, $d_{i_q}(t, i_q) = -n_p(q_a - q_k) i_d + \frac{n_p \phi_v (q_a - q_k)}{L_q}$, $g_{i_d} = -\frac{R_s i_d}{L_d}$, $b_{id} = \frac{1}{L_d}$, $d_{i_d}(t, i_d) = -n_p(q_a - q_k) i_q$.

III. LOS Stabilized Controller Design

In this section, a continuous second-order sliding mode controller based on FTDO is developed to meet the demand of fast frequency response and high precision tracking for LOS stabilized system. From system (8), the dynamics of rate and current loops have the common type, thus in this section, we take the outer rate loop controller design as an example, a detailed design process and rigorous proof are given.

Assumption 1: The disturbance $d_\omega(t, q_a)$ in (8a) is 2th order differentiable, and $\ddot{d}_\omega(t, q_a) \leq L$, where L is a known constant.

Theorem 1: For system (8a), the sliding variable $\sigma = q_{ar} - q_a$. Under Assumption 1, if the control law for rate loop is designed as

$$\begin{aligned} i_q^* = & \frac{1}{b_\omega} (\dot{q}_{ar} - g_\omega(q_a) + k_1 |\sigma|^{\frac{1}{2}} \mathrm{sign}(\sigma) \\ & + k_2 \int_0^t \mathrm{sign}(\sigma) d\tau - \hat{d}_\omega) \end{aligned} \tag{9}$$

where $k_1 > 0, k_2 > 0$, $\hat{d}_\omega = z_1$ is given by FTDO

$$\begin{aligned} & \dot{z}_0 = v_0 + g_\omega(q_a) + b_\omega i_q^*, \\ & v_0 = -\lambda_0 L^{1/3} |z_0 - q_a|^{2/3} \mathrm{sign}(z_0 - q_a)) + z_1, \\ & \dot{z}_1 = v_1, \\ & v_1 = -\lambda_1 L^{1/2} |z_1 - v_0|^{1/2} \mathrm{sign}(z_1 - v_0) + z_2, \\ & \dot{z}_2 = v_2, v_2 = -\lambda_2 L \mathrm{sign}(z_2 - v_1). \end{aligned} \tag{10}$$

Then the system output q_a will converge to the desired value q_{ar} in finite time in the presence of disturbance.

Lemma 1: [19] Suppose that the errors are defined as $e_0 = z_0 - q_a$, $e_1 = z_1 - d_\omega$,$e_2 = z_2 - \dot{d}_\omega$, then the differentiator error systems of FTDO (10) are governed by

$$\begin{aligned} & \dot{e}_0 = -\lambda_0 L^{1/3} |e_0|^{2/3} \mathrm{sign}(e_0) + e_1, \\ & \dot{e}_1 = -\lambda_1 L^{1/2} |e_1 - \dot{e}_0|^{1/2} \mathrm{sign}(e_1 - \dot{e}_0) + e_2, \\ & \dot{e}_2 \in -\lambda_2 L \mathrm{sign}(e_2 - \dot{e}_1) + [-L, L]. \end{aligned} \tag{11}$$

there exists a time constant $T \in \mathbb{R}^+$, for $\forall t > T$, $e_0 = e_1 = e_2 = 0$, that is the disturbance estimation errors converge to zero in finite time.

proof: For sliding variable σ, with the control law (9), its derivative along system trajectory(8a) is

$$\dot{\sigma} = -k_1 |\sigma|^{\frac{1}{2}} \mathrm{sign}(\sigma) - k_2 \int_0^t \mathrm{sign}(\sigma) d\tau + e_1 \tag{12}$$

Consider system dynamics (8a) and FTDO (10) as a cascaded system.

Step1: It will be shown that a bounded estimation error e_1 will not drive the sliding mode variable σ to infinity in a finite time T which is the convergence time of disturbance estimation. Define a finite-time bounded (FTB) function [21] $V_1(\sigma) = \frac{1}{2}\sigma^2$, for $\forall t \leq T$, taking the derivative of $V_1(\sigma)$ along system(12) yields

$$\begin{aligned} \dot{V}_1 &= \sigma \dot{\sigma} \\ &= -k_1 |\sigma|^{\frac{3}{2}} - k_2 \sigma \int_0^t \mathrm{sign}(\sigma) d\tau + e_1 \sigma \\ &\leq (k_2 t + e_1) \sigma \\ &\leq \frac{(k_2 T + e_1)^2}{2} + \frac{1}{2}\sigma^2 \\ &\leq K_{v_1} V_1 + L_{v_1} \end{aligned} \tag{13}$$

where $K_{v_1} = 1$ and $L_{v_1} = \frac{1}{2} \max\{(k_2 T + |e_1|)^2\}$ is bounded constant due to the boundness of e_1 from lemma 1. Then, from [21] it can be concluded that $V_1(\sigma)$ and σ will not escape in finite time T.

Step2: The sliding mode variable σ will converge to zero in finite time within the control law (9). Note that the disturbance estimation error e_1 in (11) will converge to zero in a finite time T from lemma 1. Then system (12) reduces to

$$\dot{\sigma} = -k_1 |\sigma|^{\frac{1}{2}} \mathrm{sign}(\sigma) - k_2 \int_0^t \mathrm{sign}(\sigma) d\tau \tag{14}$$

Consider the following Lyapunov function candidate

$$V_2 = \xi^{\mathrm{T}} P \xi \tag{15}$$

where

$$\begin{aligned} & \xi^{\mathrm{T}} = [|\sigma|^{\frac{1}{2}} \mathrm{sign}(\sigma), k_2 \int_0^t \mathrm{sign}(\sigma) d\tau], \\ & P = \begin{bmatrix} k_1^2 + 4k_2 & k_1 \\ k_1 & 2 \end{bmatrix}. \end{aligned}$$

With $k_1 > 0, k_2 > 0$, P is apparently positive definite. One can calculate the derivative of $V_2(\sigma)$ as

$$\dot{V}_2 = \dot{\xi}^{\mathrm{T}} P \xi + \xi^{\mathrm{T}} P \dot{\xi} \tag{16}$$

Then taking the derivative of ξ along system (14) yields

$$\begin{aligned} \dot{\xi} &= \begin{bmatrix} \frac{1}{2}|\sigma|^{-\frac{1}{2}} (-k_1 |\sigma|^{\frac{1}{2}} \mathrm{sign}(\sigma) - k_2 \int_0^t \mathrm{sign}(\sigma) d\tau) \\ k_2 \mathrm{sign}(\sigma) \end{bmatrix} \\ &= \frac{1}{2}|\sigma|^{-\frac{1}{2}} \begin{bmatrix} -k_1 & -1 \\ 2k_2 & 0 \end{bmatrix} \begin{bmatrix} |\sigma|^{\frac{1}{2}} \mathrm{sign}(\sigma) \\ k_2 \int_0^t \mathrm{sign}(\sigma) d\tau \end{bmatrix} \\ &= \frac{1}{2}|\sigma|^{-\frac{1}{2}} A \xi \end{aligned} \tag{17}$$

Submitting (17) into (16), one can obtain that

$$\dot{V}_2 = \frac{1}{2}|\sigma|^{-\frac{1}{2}}\xi^{\mathrm{T}}(A^{\mathrm{T}}P + PA)\xi = -k_1|\sigma|^{-\frac{1}{2}}\xi^{\mathrm{T}}Q\xi \tag{18}$$

where $Q = \begin{bmatrix} k_1^2 + 2k_2 & k_1 \\ k_1 & 1 \end{bmatrix}$ is positive definite.
Since $V_2(\sigma)$ is a positive definite quadratic form, then

$$\lambda_{\min}\{P\}||\xi||_2^2 \le V_2 \le \lambda_{\max}\{P\}||\xi||_2^2 \tag{19}$$

where $||\xi||_2^2 = |\sigma| + (k_2\int_0^t \mathrm{sign}(\sigma)d\tau)^2$, then we have

$$|\sigma|^{-\frac{1}{2}} \ge \frac{\lambda_{\min}^{\frac{1}{2}}\{P\}}{V_2^{\frac{1}{2}}}, ||\xi||_2^2 \ge \frac{V_2}{\lambda_{\max}\{P\}} \tag{20}$$

By using (20), (18) can be further transformed into that

$$\begin{aligned}\dot{V}_2 &\le -k_1\frac{\lambda_{\min}^{\frac{1}{2}}\{P\}}{V_2^{\frac{1}{2}}}\frac{V_2}{\lambda_{\max}\{P\}}\lambda_{\min}\{Q\} \\ &= -k_1\frac{\lambda_{\min}^{\frac{1}{2}}\{P\}\lambda_{\min}\{Q\}}{\lambda_{\max}\{P\}}V_2^{\frac{1}{2}}\end{aligned} \tag{21}$$

From the solution of (21), we can conclude that $\xi(t)$ converges to zero in finite time. In other words, the system output q_a converges to the desired value q_{ar} in finite time in the presence of disturbance $d_\omega(t, q_a)$.

Remark 1: The selections of parameters λ_i of (11) are from [19]. A possible selections here are $\lambda_0 = 2, \lambda_1 = 1.5, \lambda_2 = 1.1$. The value of L is tuned to regulate the convergence rate of the differentiator. In our method, due to the existence of term $\int \mathrm{sign}(\sigma)$, it only needs to select a relatively small value compared to the controller designed by [17].

The similar designed procedure can be realized to design two current loops. However, the control period of current loop is much less than rate loop in actual control implementation. Although the FTDO-based control method gains the excellent performance, it takes much more time cost than STW. For this reason, we choose STW control method for i_q and i_d loop controllers.

IV. Simulations Results

To demonstrate the efficiency of the proposed continuous SOSMC based on FTDO, simulations on 2-DOF inertial stabilized platform have been performed. The block diagram of the gimbal system by using dual loop cascade control are shown in Fig. 1. The parameters of gimbal system used in simulations are given as: nominal inertial matrix

$$J_{AN} = \begin{bmatrix} 0.0835 & 0 & 0 \\ 0 & 0.125035 & 0 \\ 0 & 0 & 0.0835 \end{bmatrix} \mathrm{kg}\cdot\mathrm{m}^2,$$

nominal load torque $d_N = 0.25$ N· m, the reference angular rate is $q_a = 60\,\mathrm{deg/s}$. PMSM parameters are given as: rated power $P = 400$ W, rated voltage $U = 200$ V, rated current $I_N = 2.8$ A, number of pole-pairs $n_p = 4$, armature resistance $R_s = 1.52\ \Omega$, stator inductances $L_d = L_q = L = 0.004$ H, viscous damping coefficient $B_2 = 7.403 \times 10^{-5}$ N·m·s/rad, rotor flux $\phi_v = 0.0931$ wb, rated torque $T_N = 2.0$ N·m.

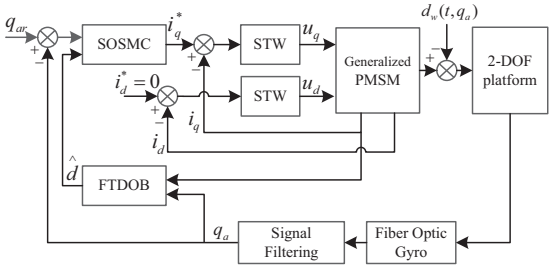

Fig. 1: The block diagram of pitch gimbal system.

TABLE I: Different Control Parameters For Rate Loop

Controllers	Parameters
PID	$K_p = 120, K_i = 4.5, K_d = 0$
SMC	$L = 120, \eta = 1.5, \varepsilon = 0.1$
FTC	$k_1 = 120, k_2 = 10$
SOSMC+FTDO	$k_1 = 120, k_2 = 2.5, L = 15$

In order to present the effectiveness of the proposed method, the traditional PID control, the SMC and FTC [13] are employed for rate loop controller for performance comparison. The different controllers are presented as follows:
(1) PID: $i_q^* = K_p\sigma + K_i\int_0^t \sigma + K_d\frac{d\sigma}{dt}$,
(2) SMC: $i_q^* = \frac{1}{b_\omega}(\dot{q}_{ar} - g_\omega(q_a) + (L+\eta)\mathrm{sat}(\sigma))$,
where $\mathrm{sat}(\sigma) = \begin{cases} \dfrac{\sigma}{||\sigma||}, & ||\sigma|| \ge \varepsilon, \\ \dfrac{\sigma}{\varepsilon}, & ||\sigma|| < \varepsilon. \end{cases}$
(3) FTC: $i_q^* = \frac{1}{b_\omega}(\dot{q}_{ar} - g_\omega(q_a) + k_1|\sigma|^{\frac{1}{2}}\mathrm{sign}(\sigma) + k_2\sigma)$.

To have a fair comparison, the control inputs of various methods have the same saturation limits $|i_q^*|_{\max} = 5.0$ A and the STW control method is chosen for the current loop.

For rate loop, the parameters of all the four control methods are listed in Table I. Simulation studies are carried out in the presence of cross coupling torque caused by vehicle motion, mass unbalance and parameter perturbations and unknown external load disturbances in a Gaussian noise environment.

Case 1: Simulation results in the presence of cross coupling torque. Suppose that the angular rate of vehicle motion or frame B is $\Omega_B = [0, 25\sin 2\pi t, 25\cos 2\pi t]^{\mathrm{T}}\,\mathrm{deg/s}$, relative angle and angular rate of yaw gimbal or frame K are $v_1 = 15t\,\mathrm{deg}, \dot{v}_1 = 15\,\mathrm{deg/s}$ at $t = 1$ s, respectively. Due to the mass unbalance, the inertial matrix is set as $J_A = J_{AN} + \Delta J_A$, where

$$\Delta J_A = \begin{bmatrix} 0.0148 & -0.0329 & -0.0468 \\ -0.0329 & 0.0245 & 0.0375 \\ -0.0468 & 0.0375 & 0.0185 \end{bmatrix} \mathrm{kg}\cdot\mathrm{m}^2,$$

The simulation results in this case are shown in Fig. 2-4.

As shown by Fig. 2, the cross coupling torque caused by motion and mass unbalance is estimated completely in finite time by FTDO. Fig. 3 shows that the proposed SOSMC based on FTDO can remove the offset caused by external disturbances. On the contrary, the tracking error increases with the disturbance amplitude by the other methods. And the

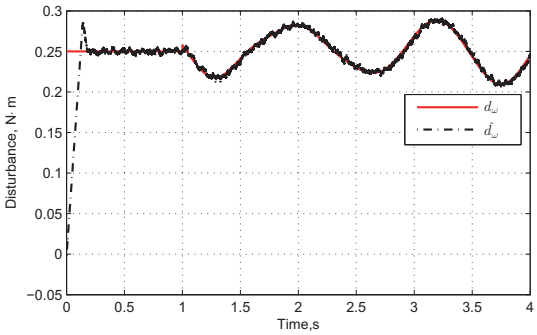

Fig. 2: Response curves of disturbance estimation $\hat{d}_\omega$.

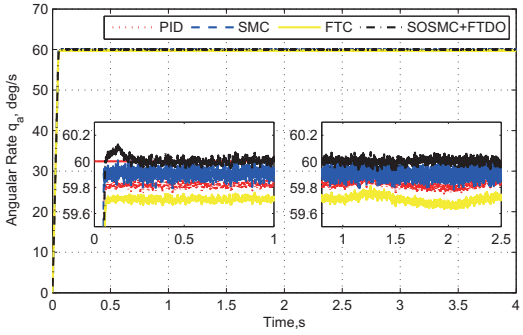

Fig. 3: Response curves of angular rate q_a of pitch gimbal with cross coupling torqued disturbance under four controllers.

discontinuous term of traditional SMC methods leads to the highest ripple among four methods though the switch function has replaced by saturation function. In Fig. 4d, it shows that SOSMC does not lead to any chattering phenomenon due to its continuous control action.

Case 2: Simulation results in the presence of external uncertain load torque. In practical applications, uncertain load torque contains many aspects such as weight of optical electronic tracker, cable restraint, wind drag torque, et al. In this case, we make an assumption that the lumped uncertain load torque $d_e(t, q_a) = (0.35\sin(\pi t) + 0.1 + d_N)$ N· m to imitate the real engineering, and 2-DOF gimbal system have no mass unbalance and the frame B and K are still, i.e., the crossing torque is ignored. The simulation results in this case are shown in Fig. 5-7.

As shown by Fig. 6, with the load variation, the proposed methods obtains better dynamic performance compared to the others. The rest comparison results are similar to Case 1, which demonstrates that the control scheme based on disturbance compensation is suitable and effective to 2-DOF ISP.

V. Conclusions

A continuous second-order sliding mode control based on FTDO for LOS stabilized loop is presented in this paper. The nonlinear disturbances of 2-DOF gimbal system including coupling torque, mass unbalance torque and uncertain load torque

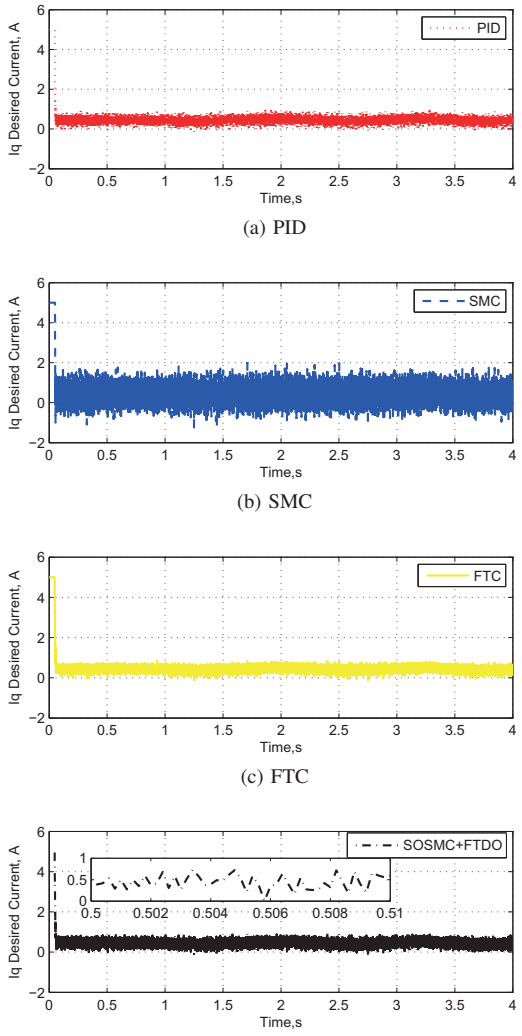

(a) PID

(b) SMC

(c) FTC

(d) SOSMC+FTDO

Fig. 4: Response curves of input i_q current with cross coupling torqued disturbance under four controllers.

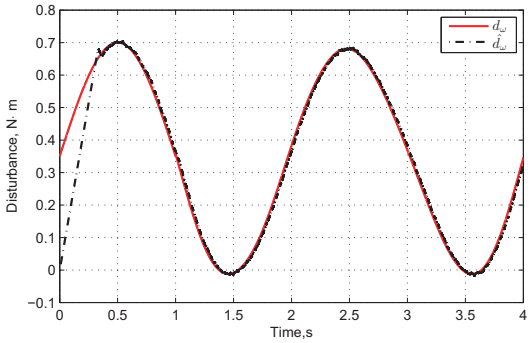

Fig. 5: Response curves of disturbance estimation $\hat{d}_\omega$.

are estimated by the observer for a feedforward compensation control. With the proposed control approach, the tracking error

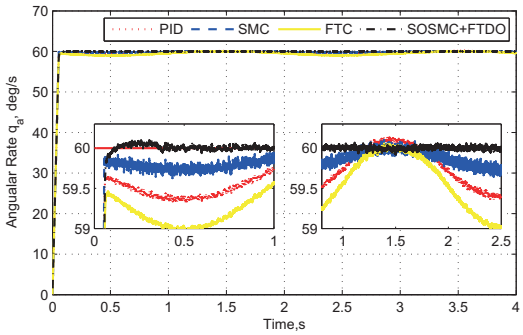

Fig. 6: Response curves of angular rate q_a of pitch gimbal with external uncertain load disturbances under four controllers.

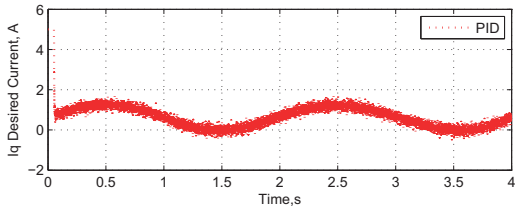

(a) PID

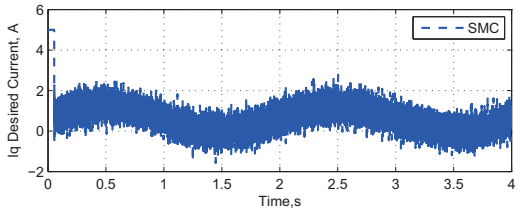

(b) SMC

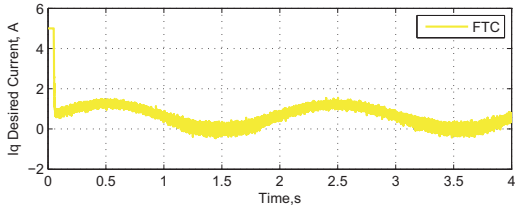

(c) FTC

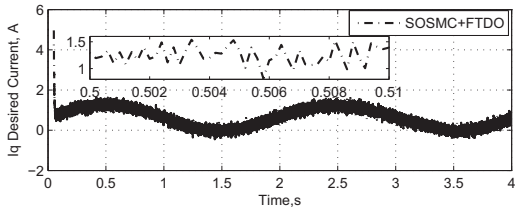

(d) SOSMC+FTDO

Fig. 7: Response curves of input i_q current with external uncertain load disturbances under four controllers.

of angular rate can converge to zero in finite time in the presence of the disturbances. The simulation results show that the proposed method exhibits much better static and dynamic performances compared with the traditional PID control, SMC and FTC methods.

ACKNOWLEDGMENT

The authors would like to thank the foundation of International Science & Technology Cooperation Program of China (2015DFA10490) and the Fundamental Research Funds for the Central Universities and the Innovate Foundation for Graduate Student of JiangSu Province (KYLX15_0213).

REFERENCES

[1] J. Hilkert, Inertially stabilized platform technology concepts and principles, *IEEE Control Systems Magazine*, 2008, 28(1): 26-46.

[2] B. Ekstrand, Equations of motion for a two-axes gimbal system, *IEEE Transactions on Aerospace and Electronic Systems*, 2001, 37(3): 1083-1091.

[3] H. Khodadadi, M. Motlagh, M. Gorji, Robust control and modeling a 2-DOF Inertial Stabilized Platform, in *Proceedings of International Conference on Control and Computer Engineering (INECCE)*, 2011: 223-228.

[4] W. Ji, Q. Li, B. Xu, et al, Adaptive fuzzy PID composite control with hysteresis-band switching for line of sight stabilization servo system, *Aerospace Science and Technology*, 2011, 15(1): 25-32.

[5] J. Moorty, R. Marathe, H∞ control law for line-of-sight stabilization for mobile land vehicles, *Optical engineering*, 2002, 41(11): 2935-2944.

[6] X. Zhou, H. Zhang, R. Yu, Decoupling control for two-axis inertially stabilized platform based on an inverse system and internal model control, *Mechatronics*, 2014, 24(8): 1203-1213.

[7] J. Fang, R. Yin, X. Lei, An adaptive decoupling control for three-axis gyro stabilized platform based on neural networks, *Mechatronics*, 2015, 27: 38-46.

[8] H. Liu, S. Li, Speed control for PMSM servo system using predictive functional control and extended state observer, *IEEE Transactions on Industrial Electronics*, 2012, 59(2): 1171-1183.

[9] S. Li, Z. Liu, Adaptive speed control for permanent-magnet synchronous motor system with variations of load inertia, *IEEE Transactions on Industrial Electronics*, 2009, 56(8): 3050-3059.

[10] S. Li, M. Zhou, X. Yu, Design and implementation of terminal sliding mode control method for PMSM speed regulation system, *IEEE Transactions on Industrial Informatics*, 2013, 9(4): 1879-1891.

[11] S. Li, H. Liu, S. Ding, A speed control for a PMSM using finite-time feedback control and disturbance compensation, *Transactions of the Institute of Measurement and Control*, 2010, 32(2): 170-187.

[12] Y. Feng, X. Yu, Z. Man, Non-singular terminal sliding mode control of rigid manipulators, *Automatica*, 2002, 38(12): 2159-2167.

[13] S. Yu, X. Yu, B. Shirinzadeh, et al, Continuous finite-time control for robotic manipulators with terminal sliding mode, *Automatica*, 2005, 41(11): 1957-1964.

[14] W. Chen, Disturbance observer based control for nonlinear systems, *IEEE/ASME Transactions on Mechatronics*, 2004, 9(4): 706-710.

[15] W. Chen, J. Yang, L. Guo, et al, Disturbance observer-based control and related methods: An overview, *IEEE Transactions on Industrial Electronics*, 2015, 63(2): 1083 - 1095.

[16] Y. Shtessel, I. Shkolnikov, A. Levant, Smooth second-order sliding modes: Missile guidance application, *Automatica*, 2007, 43(8): 1470-1476.

[17] J. Yang, S. Li, J. Su, et al, Continuous nonsingular terminal sliding mode control for systems with mismatched disturbances, *Automatica*, 2013, 49(7): 2287-2291.

[18] S. He, D. Lin, J. Wang, Continuous second-order sliding mode based impact angle guidance law, *Aerospace Science and Technology*, 2015, 41: 199-208.

[19] A. Levant, Higher-order sliding modes, differentiation and output-feedback control, *International Journal of Control*, 2003, 76(9-10): 924-941.

[20] Y. Shtessel, M. Taleb, F. Plestan, A novel adaptive-gain supertwisting sliding mode controller: methodology and application. *Automatica*, 2012, 48(5): 759-769.

[21] S. Li, Y. Tian, Finite-time stability of cascaded time-varying systems, *International Journal of Control*, 2007, 80(4): 646-657.